Comparison of Daytime Low-Level Cloud Properties Derived from GOES and ARM SGP Measurements

Theodore M. McHardy[1], Xiquan Dong[1], Baike Xi[1], Mandana M. Thieman[2], Patrick Minnis[3], and Rabindra Palikonda[2]

1. Department of Hydrology and Atmospheric Sciences, University of Arizona, Tucson, AZ
2. SSAI, Inc. Hampton, VA
3. NASA Langley Research Center, Hampton, VA

Publications supported by CERES in 2017

Papers published

- Huang Y, **X, Dong**, B. Xi, E.K. Dolinar, R.E. Stanfield and S. Qiu, 2017: Quantifying the uncertainties of reanalyzed Arctic cloud and radiation properties using satellite-surface observations: J Clim., 8007-8029, 30, 10.1175/JCLI-D-16-0722.1
- Huang, Y., **X. Dong**, B. Xi, E. Dolinar, R. Stanfield, 2017: The footprints of 16-year trends of Arctic springtime cloud and radiation properties on September sea-ice retreat. JGR. 122, 2179-2193. DOI: 10.1002/2016JD026020
- Wu, P., **X. Dong**, B. Xi, Y. Liu, M. Khaiyer, and P. Minnis, 2017: Effects of Environment Forcing on Marine Boundary Layer Cloud-Drizzle Processes. JGR-atmosphere, 122, 4463-4478, doi:10.1002/2016JD026326
- Zhang, Z., **X. Dong**, B. Xi, H. Song, P-L. Ma, S. Ghan, S. Platnick, and P. Minnis, 2017: Inter-comparisons of marine boundary layer cloud properties from two MODIS products and ground-based retrievals over the ARM Azores site. JGR. 122, DOI:10.1002/2016JD025763.

Papers submitted

- Tian, J., **X. Dong**, B. Xi, P. Minnis, S. Sun-Mack[4] and W. L. Smith, Jr., 2017: Comparisons of Water Path in Deep Convective Systems among CERES-MODIS, GOES, and Ground-based retrievals. Submitted to JGR.
- Qiu S., **X. Dong** and B. Xi, 2017: Arctic boundary layer properties and its relationship with cloud occurrence frequency, phase and structure in autumn season. Submitted to JGR.
- McHardy, T.M., **X. Dong**, B. Xi, M. M. Thieman, and P. Minnis, 2017: Comparison of Daytime low- level Cloud Properties derived from GOES and ARM SGP Measurements. Submitted to JGR.

- **Purpose:**
  - To statistically characterize GOES cloud property retrievals (VISST/CERES algorithm, Minnis et el., 2008, 2011) of low-level water clouds over land vs. ARM ground-based observations and retrievals during a 8-yr period.
- **Motivation:**
  - As new versions are released, products need to be re-evaluated
  - Stratocumulus over land are understudied compared to marine stratocumulus

Data and Results

.GOES VISST Pixel level (4km x 4km) available on ARM data archive (every half hour)

.DOE ARM SGP surface data (every 5 min.)

.6/1998 – 12/2006

Satellite	Position	Period	Version
GOES 8	East	05/01/1998 – 12/31/1998	2.1
		01/01/1999 – 12/31/1999	2.1
		01/01/2000 – 03/30/2003	3
GOES 10	West	04/01/2003 – 08/31/2005	3
		09/01/2005 – 06/20/2006	2.1
GOES 11	West	06/21/2006 – 12/31/2006	3

[Ellingson et al., 2001]

Data Processing

- **Collocation:**
  - GOES data spatially averaged within 0.3°x0.3° box centered on the ARM SGP site (~ 36.6N, 97.5W)
  - ARM data temporally averaged ±15 min of GOES scan (no overlap)
- **Data Filters (to allow only low-level water clouds):**
  - Solar Zenith Angle < 78°
  - Identified by MMCR as low-level clouds (top < 3 km)
  - ARM cloud base temp. > 250K
  - GOES cloud fraction = 1
  - ARM H_{top} values within 500m (for each GOES scan)
  - For each GOES box $\boldsymbol{std.dev(Teff)/mean(Teff) < 0.015}$

July and August low sample size

12z and 24z low data counts due to SZA filter

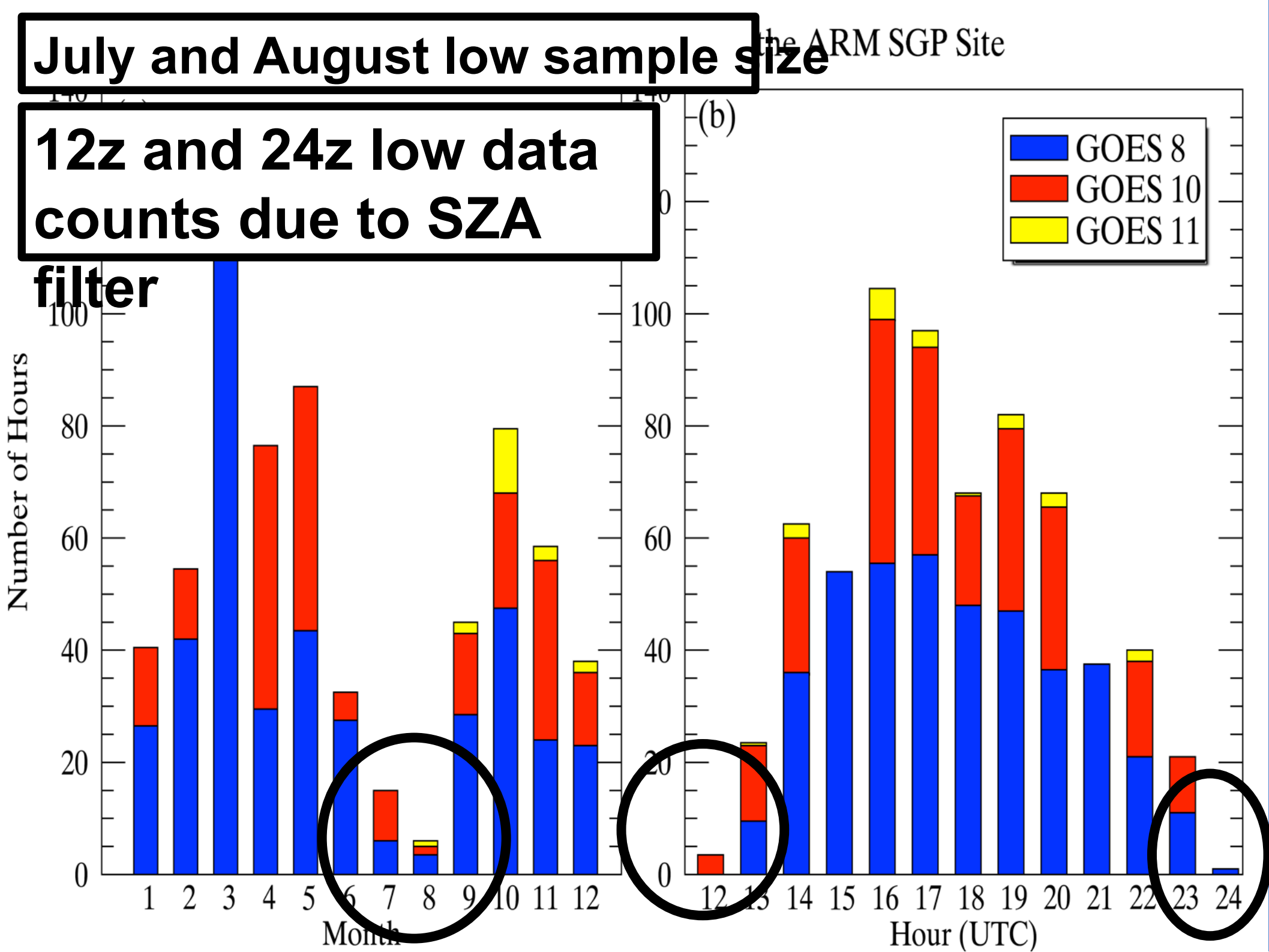

Part I

Cloud Temp. and Height Comparisons

a) Monthly means
b) Hourly means

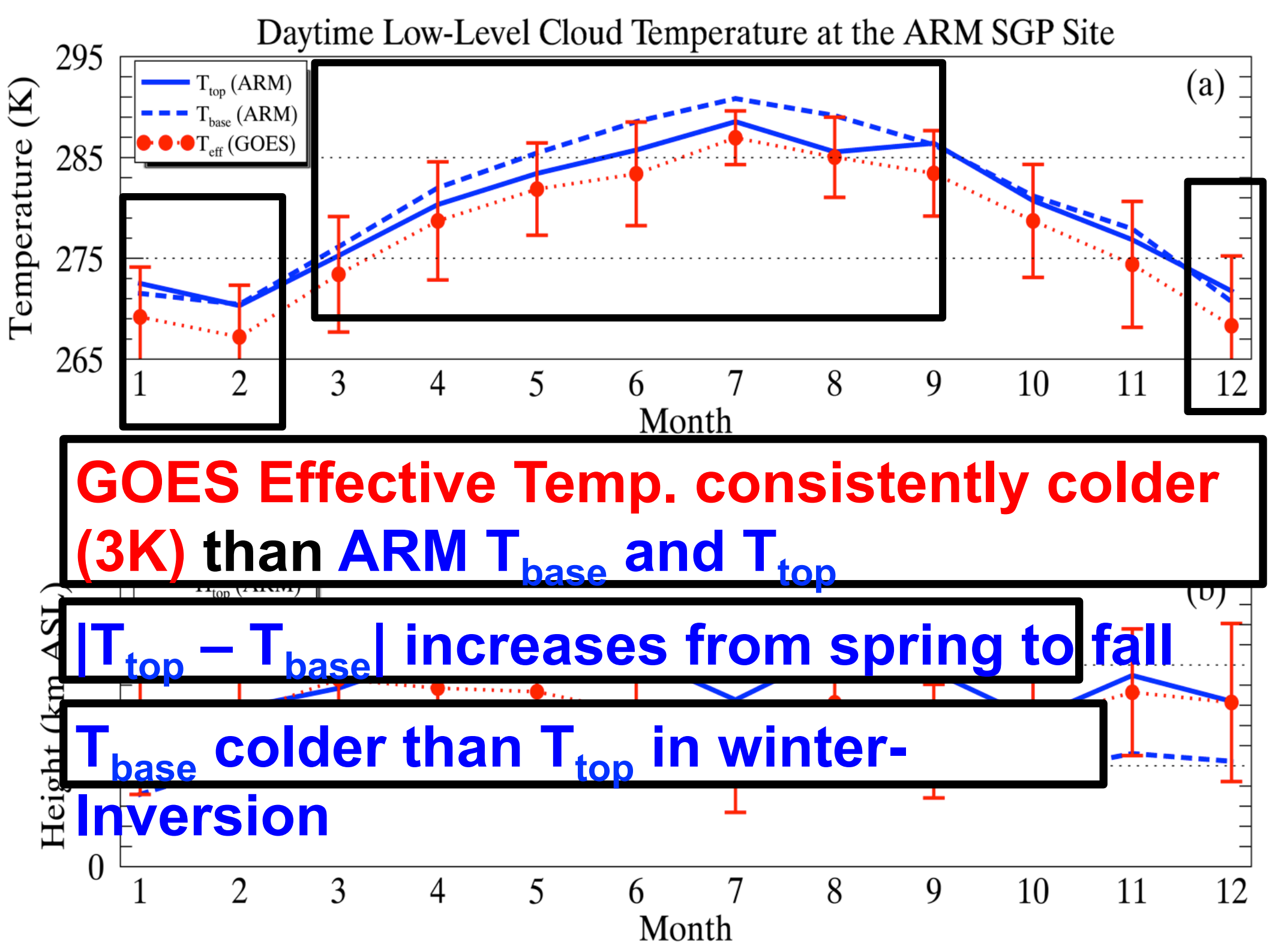
Daytime Low-Level Cloud Temperature at the ARM SGP Site
Temperature (K)
295
285
275
265
T_{top} (ARM)
T_{base} (ARM)
T_{eff} (GOES)
(a)
1
2
3
4
5
6
7
8
9
10
11
12
Month
GOES Effective Temp. consistently colder (3K) than ARM T_{base} and T_{top}
$|T_{top} - T_{base}|$ increases from spring to fall
T_{base} colder than T_{top} in winter-Inversion
Height (km ASL)
0
(b)
Month

GOES Effective Height near cloud base in summer

GOES Effective Height near cloud top from late fall to early spring

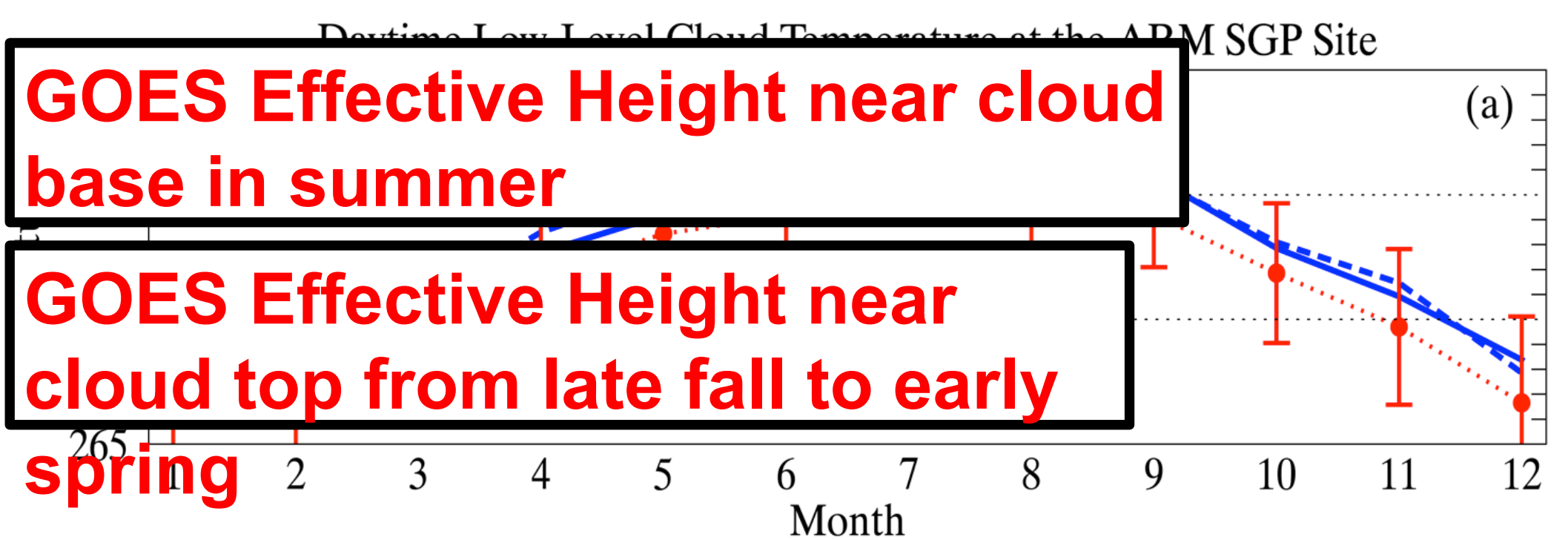

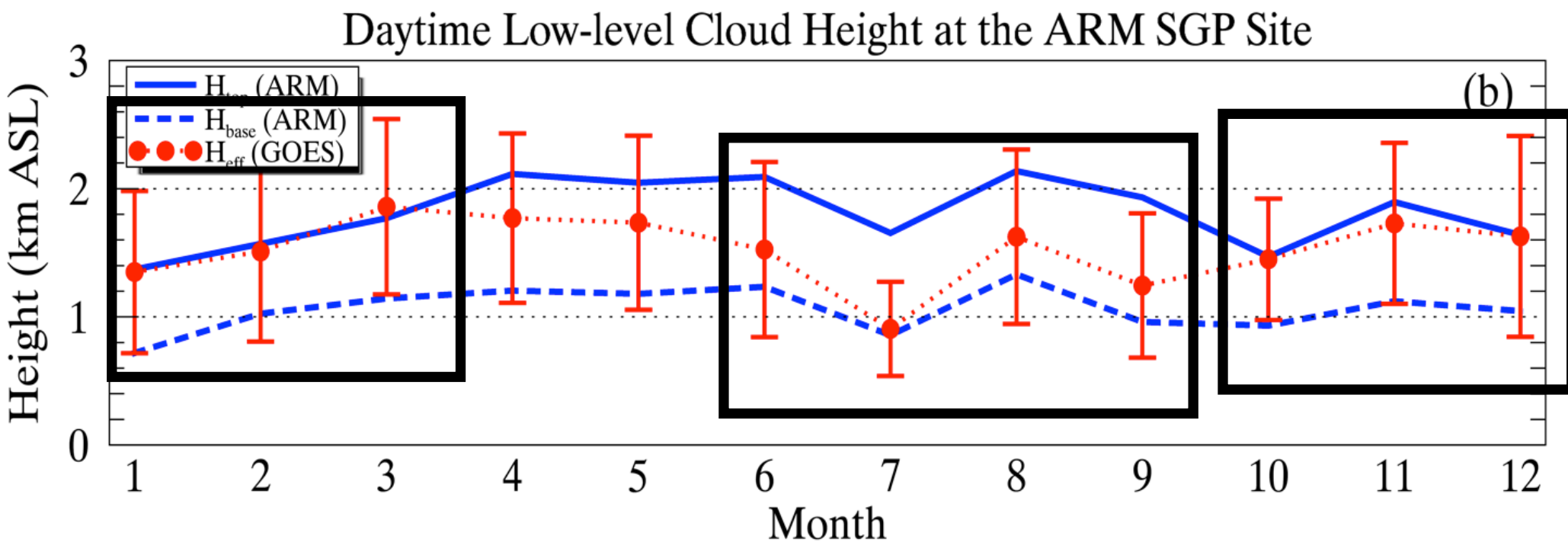

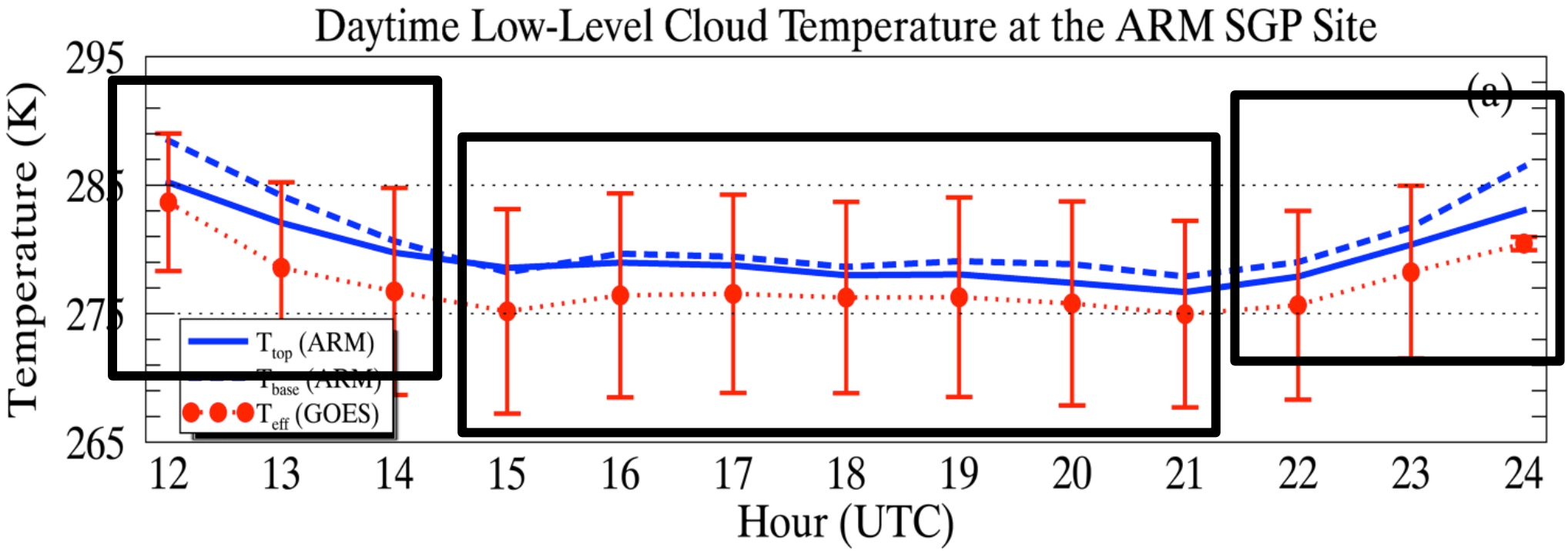

GOES Effective Temp fairly consistent

Sampling bias (mostly occurring during the summer) due to SZA filter

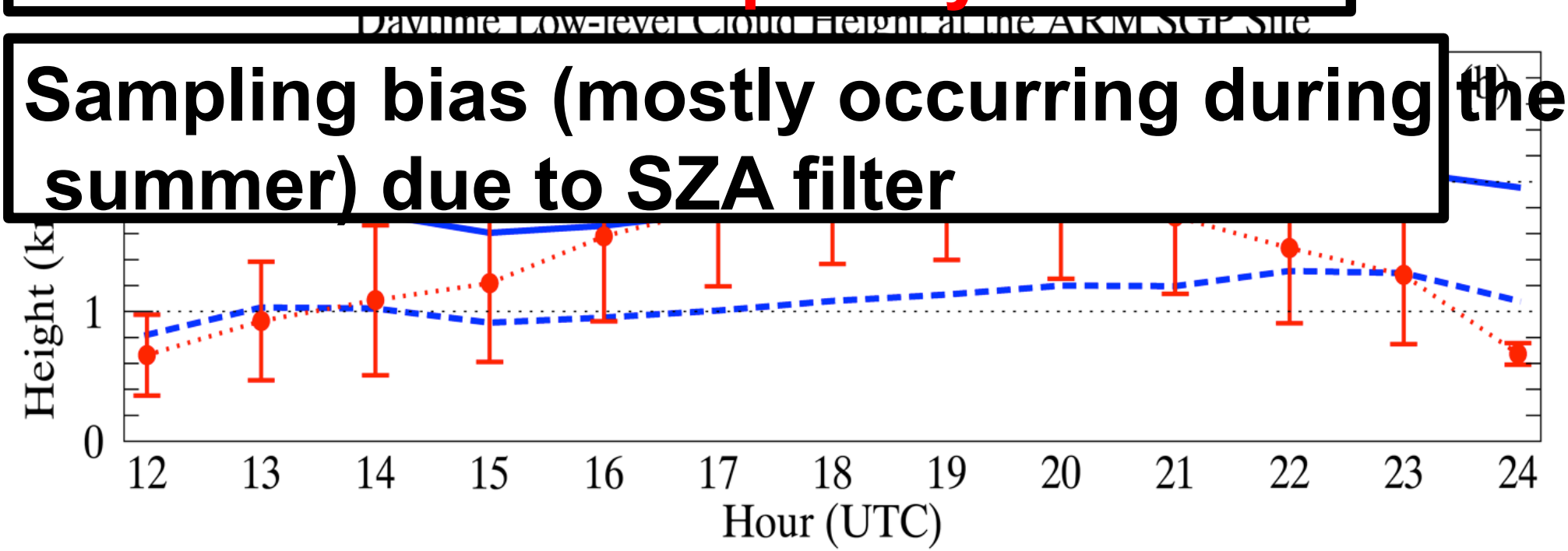

ARM H_{top} and H_{base} increase slightly throughout Day due to PBL heats up

GOES H_{eff} peaks around local noon – error due to being anchored to surface temp T_{sfc}

$$H_{eff}=[T_{sfc}-T_{eff}]/\Gamma$$

This has been changed in newer versions .

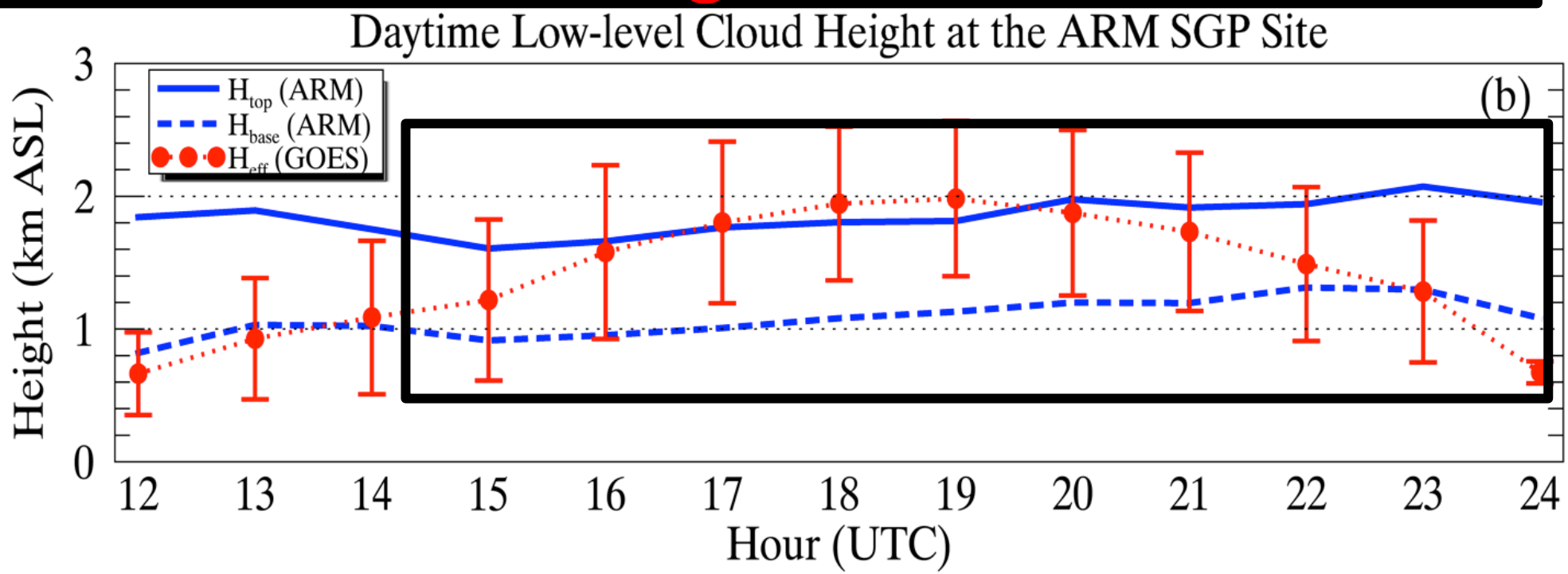

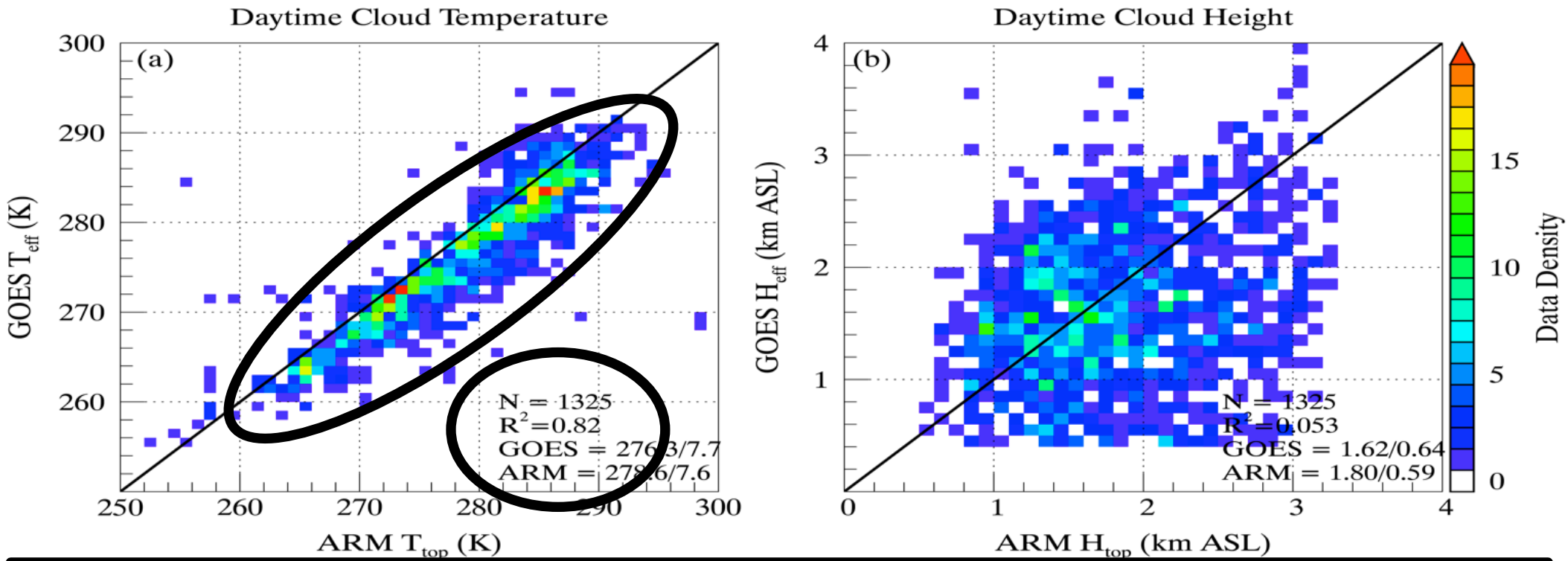

T_{eff} (GOES) and T_{top} (ARM) well correlated R^2 =

T_{eff} cold bias seen in scatter density (not unexpected due to nature of T_{eff} (GOES) vs T_{top} (ARM)), however it is colder than seen in over-ocean studies e.g. Xi et al., [2014] and Painemal and Zuidema [2011].

Painemal [2013] hypothesized the cold bias is due

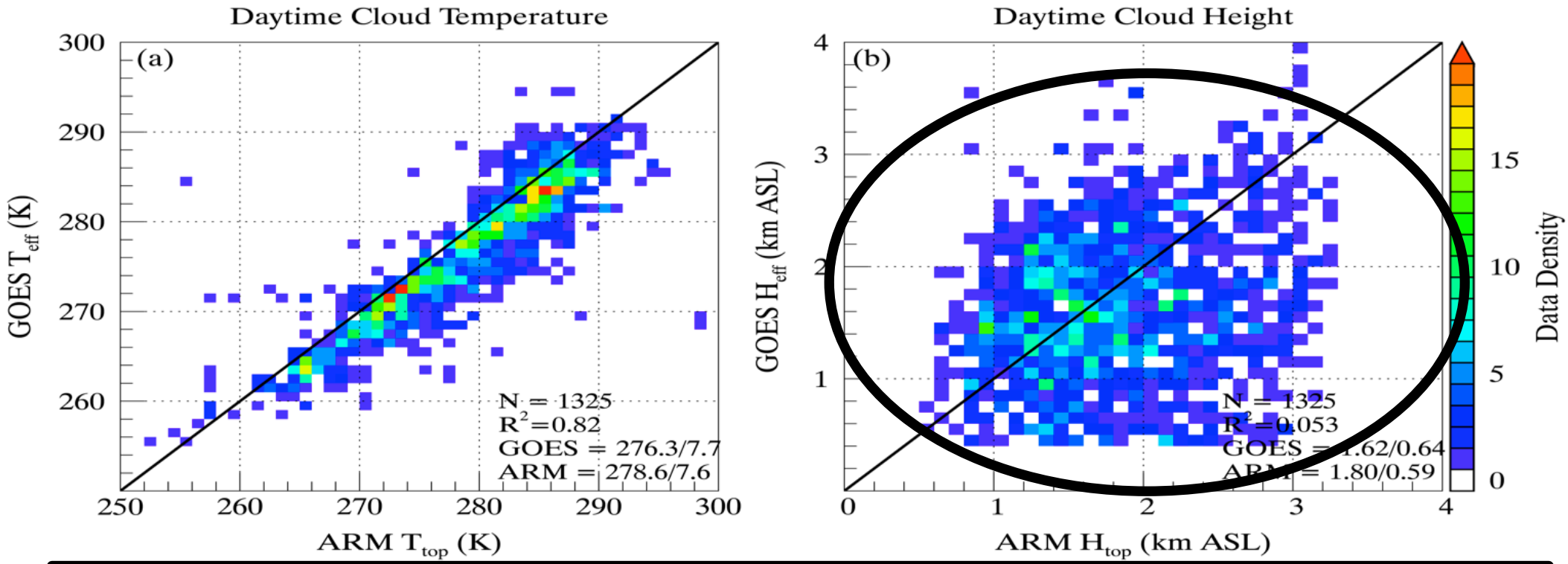

PDF

H_{eff} (GOES) and H_{top} (ARM) not correlated (R^2 = 0.053) for two reasons:

- **H_{eff} (GOES) and H_{top} (ARM) are fundamentally different quantities**
- **As mentioned, error in H_{eff} algorithm due to surface temp. dependency**

Part II

Cloud Microphysics Comparisons

a) Monthly means
b) Hourly means

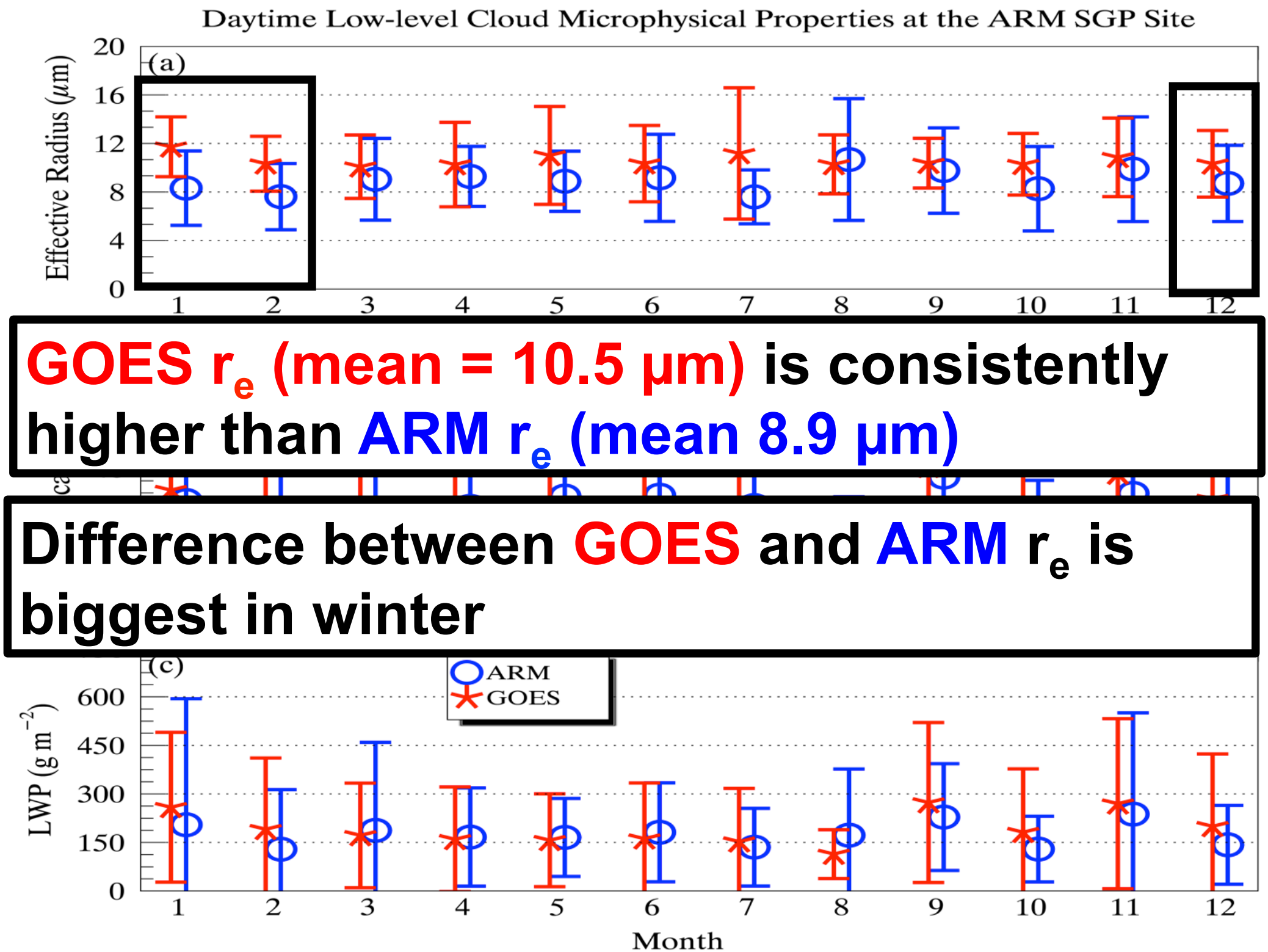

GOES r_e (mean = 10.5 μm) is consistently higher than ARM r_e (mean 8.9 μm)

Difference between GOES and ARM r_e is biggest in winter

GOES τ and LWP follow the pattern of ARM fairly well

GOES τ and LWP standard deviations higher in fall/winter

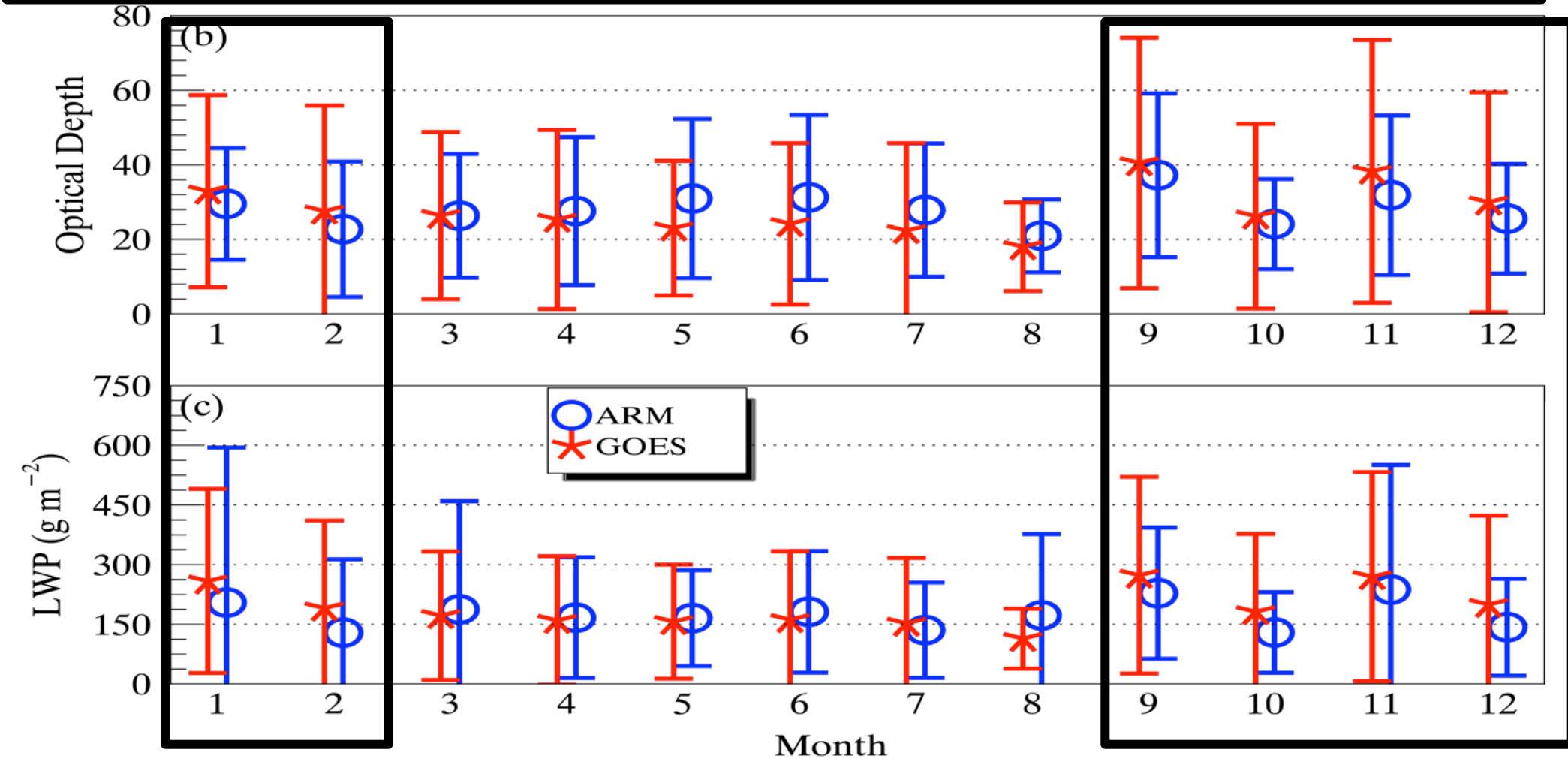

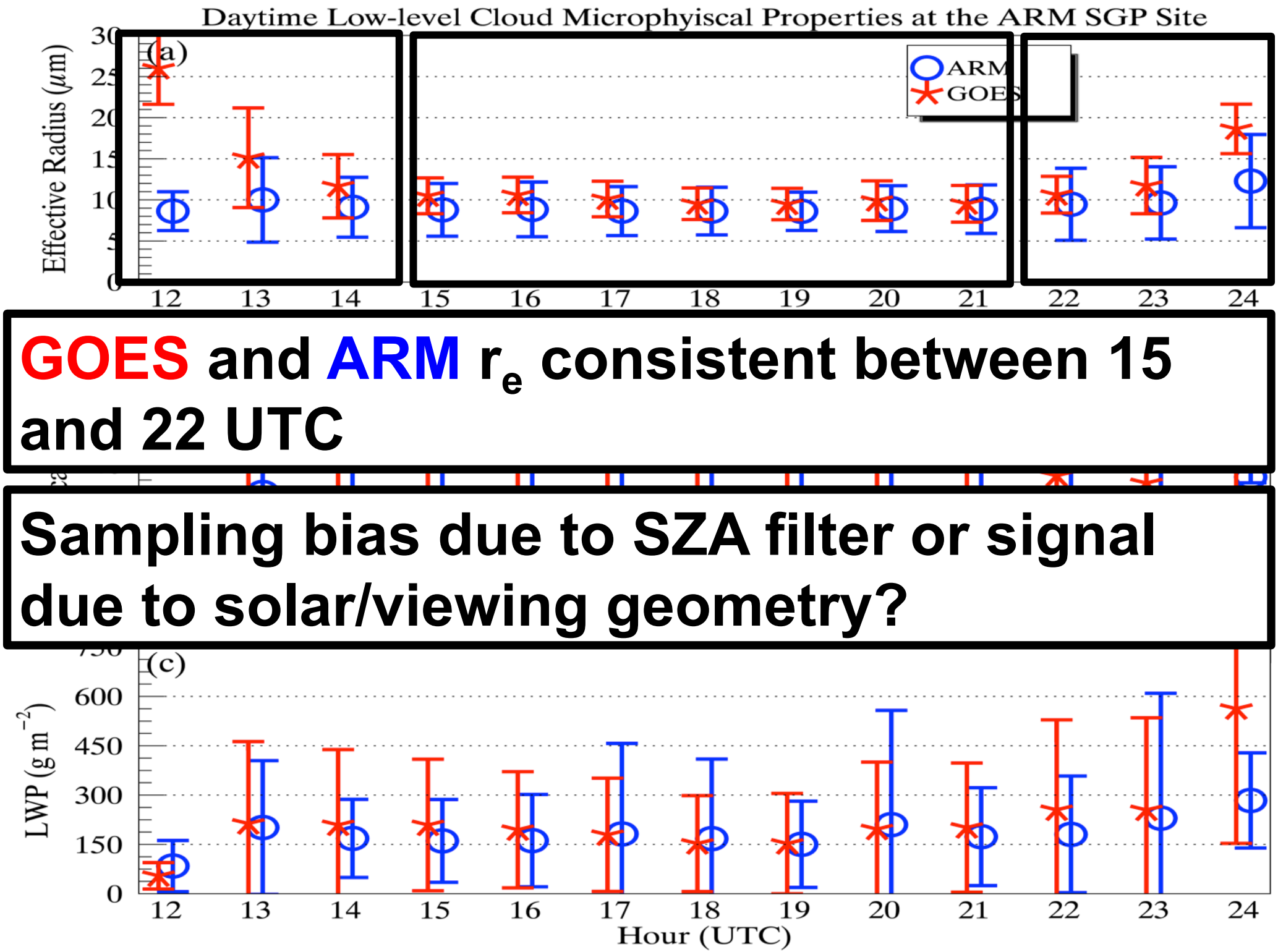

GOES and ARM r_e consistent between 15 and 22 UTC

Sampling bias due to SZA filter or signal due to solar/viewing geometry?

τ and LWP similar, though less pronounced, patterns as r_e – relatively constant throughout the day (12 UTC has a very low sample size) and peaking towards sunset

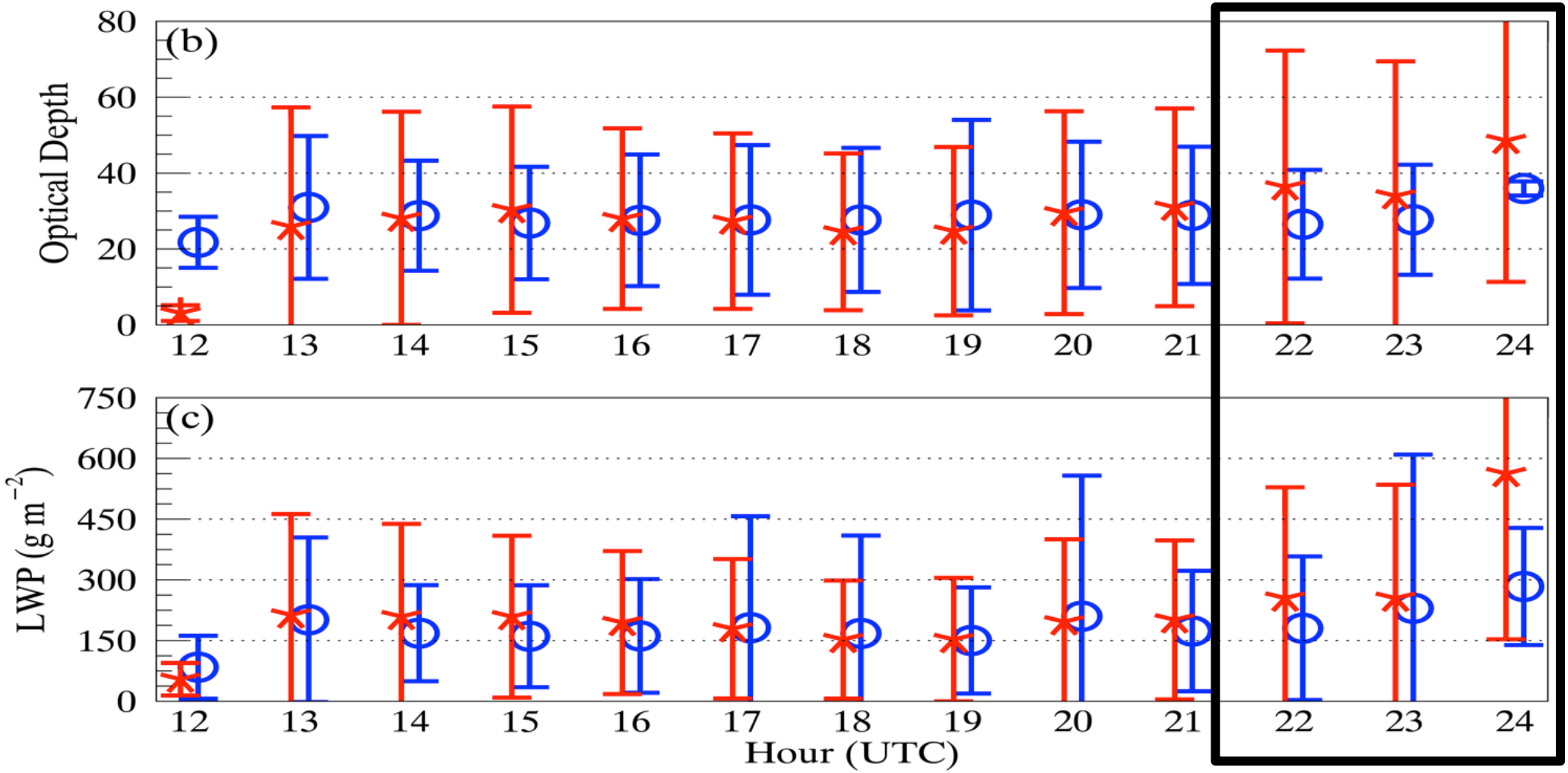

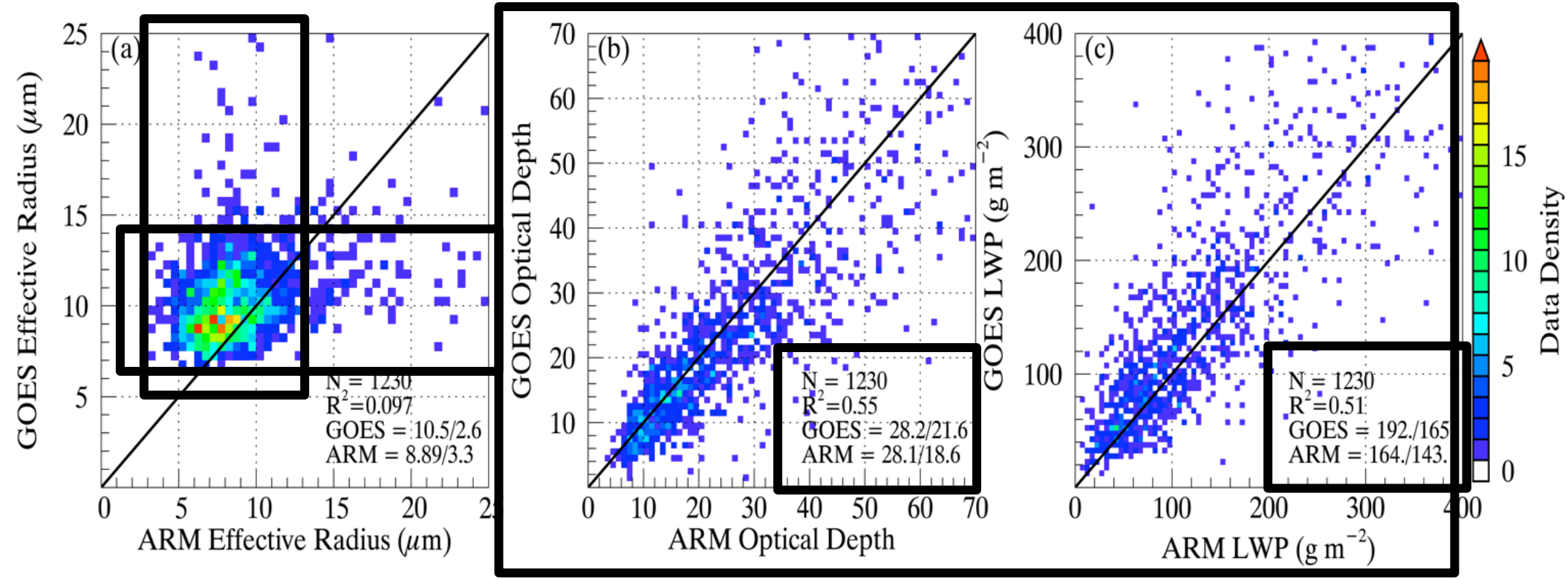

LWP (R^2 = 0.51) and τ (R^2 = 0.55) well correlated, with a moderate amount of

GOES LWP has a high bias (mean = 192 g m^{-2} vs ARM mean 164 g m^{-2}); τ means differ by 0.1

r_e (R^2 = 0.1) not correlated, with two noticeable nodes

Dependency of microphysical retrievals on SZA

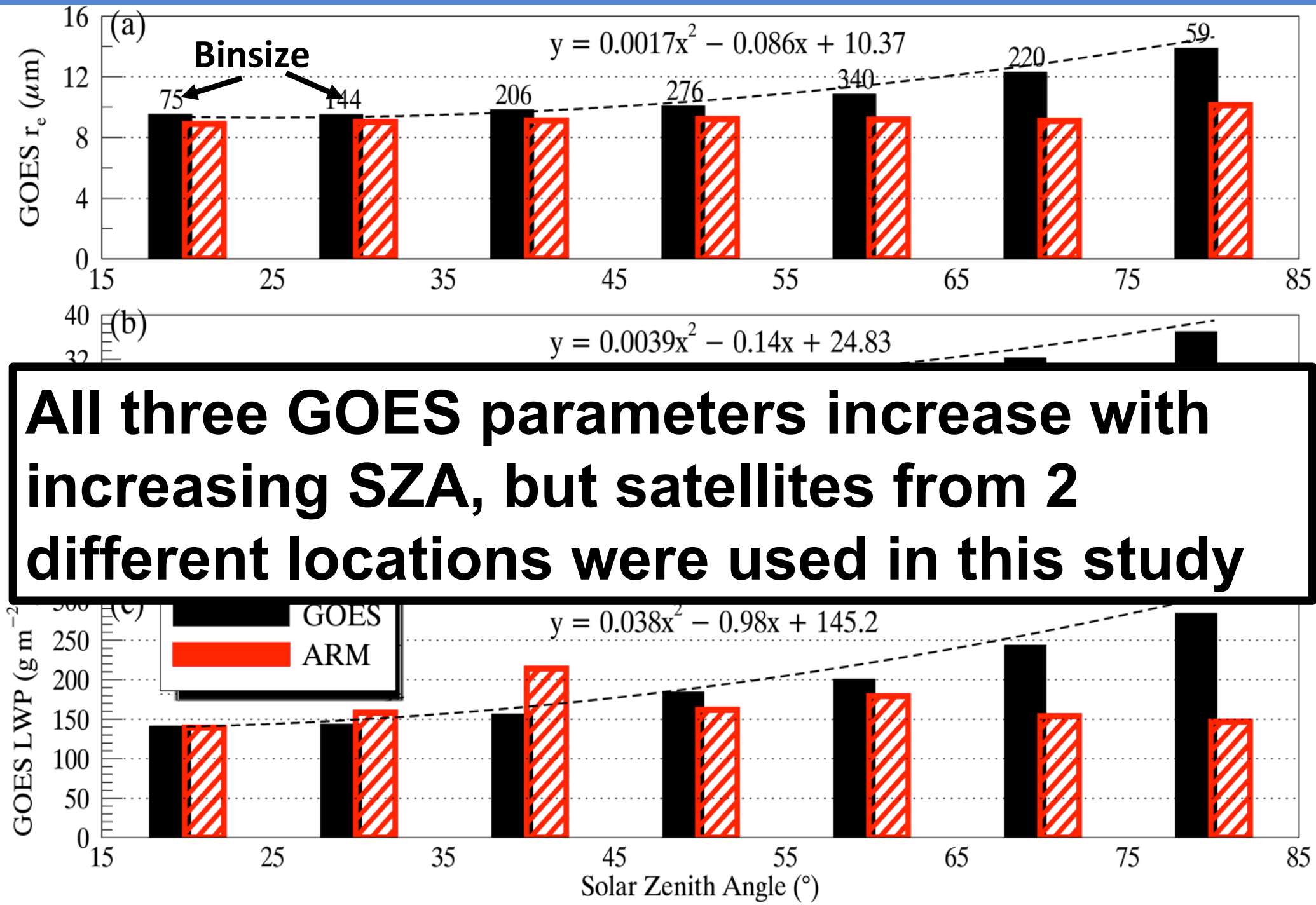

All three GOES parameters increase with increasing SZA, but satellites from 2 different locations were used in this study

Dependency on Scattering Angle (SCA)

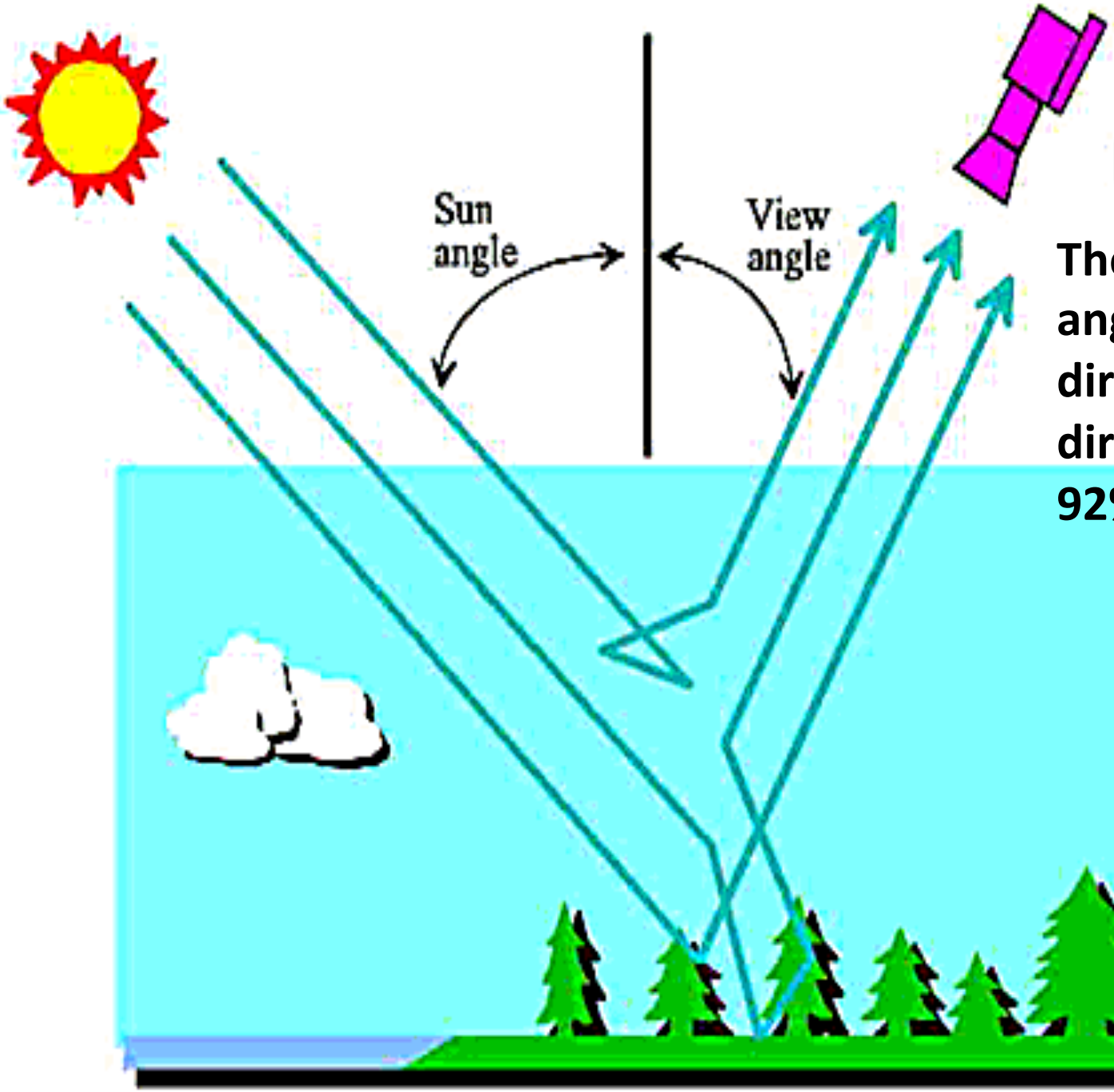

The scattering angle is the angle between the sun's direction and the viewing direction.

92% GOES data at SCA >90°

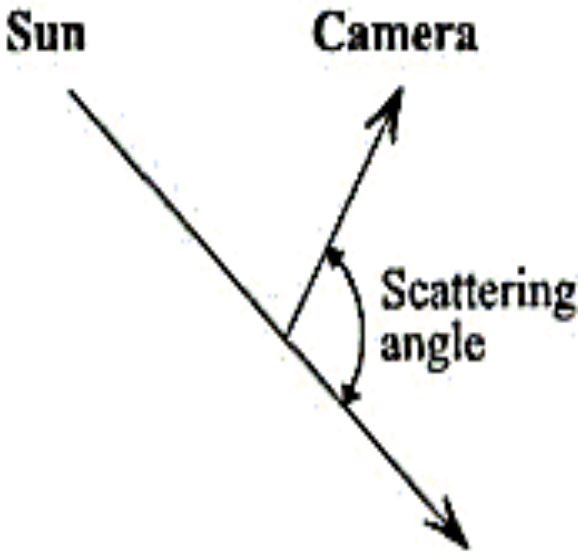

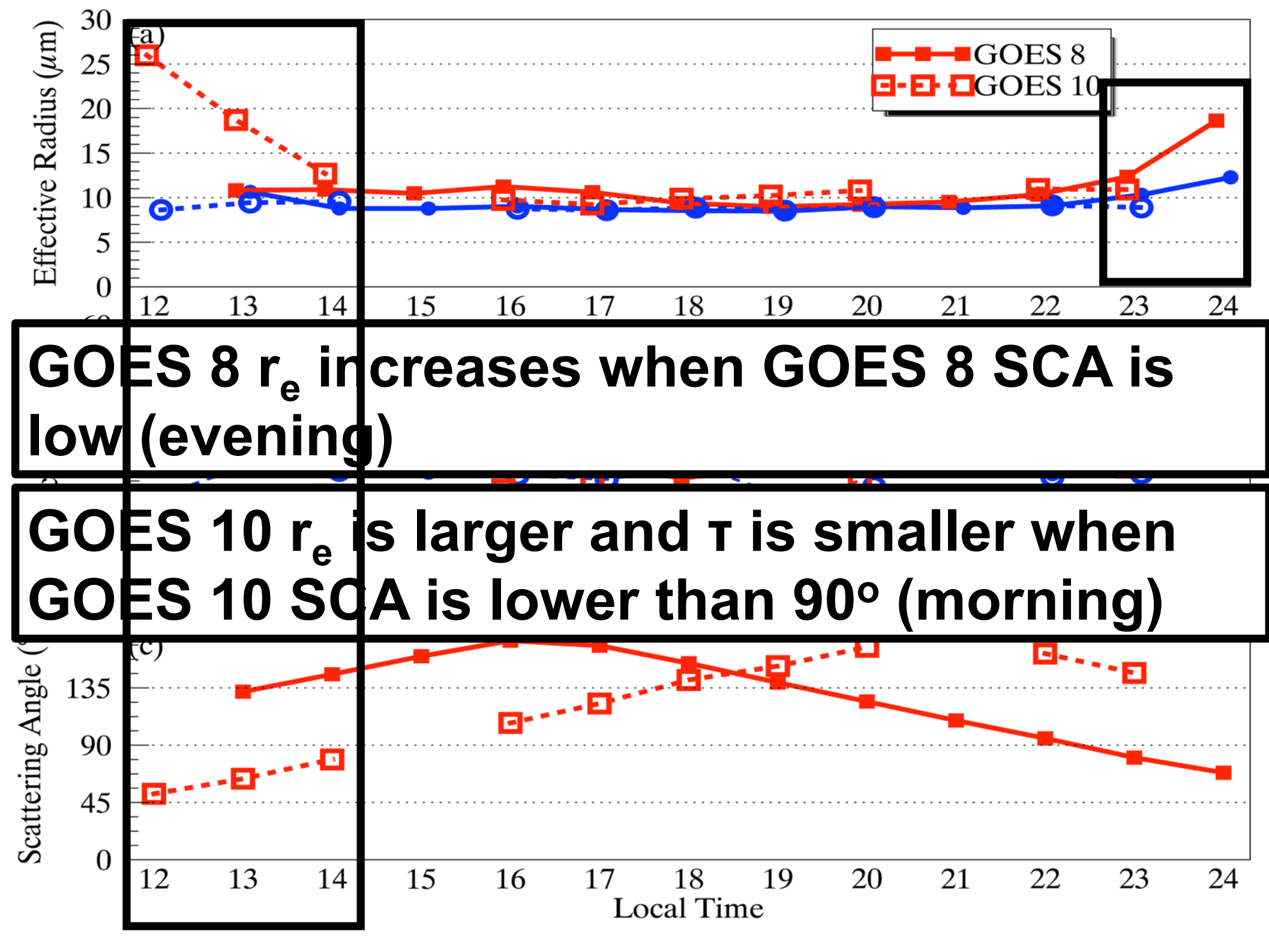

GOES 8 r_e increases when GOES 8 SCA is low (evening)

GOES 10 r_e is larger and τ is smaller when GOES 10 SCA is lower than 90° (morning)

Conclusions

- T_{eff} (GOES) and T_{top} (ARM) well correlated (R^2 = 0.82), but T_{eff} cold bias is colder than seen in over-ocean, due to evaporation and LW cooling of droplets at cloud top.
- H_{eff} (GOES) and H_{top} (ARM) not correlated (R^2 = 0.053), due to H_{eff} algorithm depending on surface temp.
- LWP (R^2 = 0.51) and τ (R^2 = 0.55) well correlated, with a moderate amount of scatter and GOES LWP has a high bias.
- When SCA<90° and SZA>65°, GOES r_e is overestimated but τ is underestimated.

References

- *Xi, B., X. Dong, P. Minnis, and S. Sun-Mack (2014), Comparison of marine boundary layer cloud properties from CERES-MODIS Edition 4 and DOE ARM AMF measurements at the Azores, J. Geophys. Res. Atmos., 119, 9509–9529, doi: 10.1002/2014JD021813.*
- Sun-Mack, S., P. Minnis, Y. Chen, S. Kato, Y. Yi, S. C. Gibson, P. W. Heck and D. M. Winker (2014), Regional apparent boundary layer lapse rates determined from CALIPSO and MODIS data for cloud-height determination. *Journal of Applied Meteorology and Climatology*, *53*(4), 990-1011.
- Painemal, D., P. Minnis, and L. O'Neill (2013), The diurnal cycle of boundary layer height and cloud cover over the Southeast Pacific as observed by GOES-10, *J. Atmos. Sci.*, **70**, 2393-2408, doi:10.1175/JAS-D-12-0325.1.
- *Minnis, P., et al. (2011), CERES Edition-2 cloud property retrievals using TRMM VIRS and Terra and Aqua MODIS data, Part I: Algorithms, IEEE Trans. Geosci. Remote Sens., 99, 1–27, doi:10.1109/TGRS.2011.2144601.*
- Minnis, P., et al. (2008b), Near-real time cloud retrievals from operational and research meteorological satellites, *Proc. SPIE Remote Sens. Clouds Atmos. XIII*, *7107-2*, Cardiff, Wales, UK, 15-18 September, 8 pp., ISBN: 9780819473387.
- *Loeb, N. G., T. Varnai, and D. M. Winker (1998), Influence of sub-pixel scale cloud-top structure on reflectances from overcast stratiform clouds, J. Atmos. Sci., 55, 2960-2973.*

Extra slides

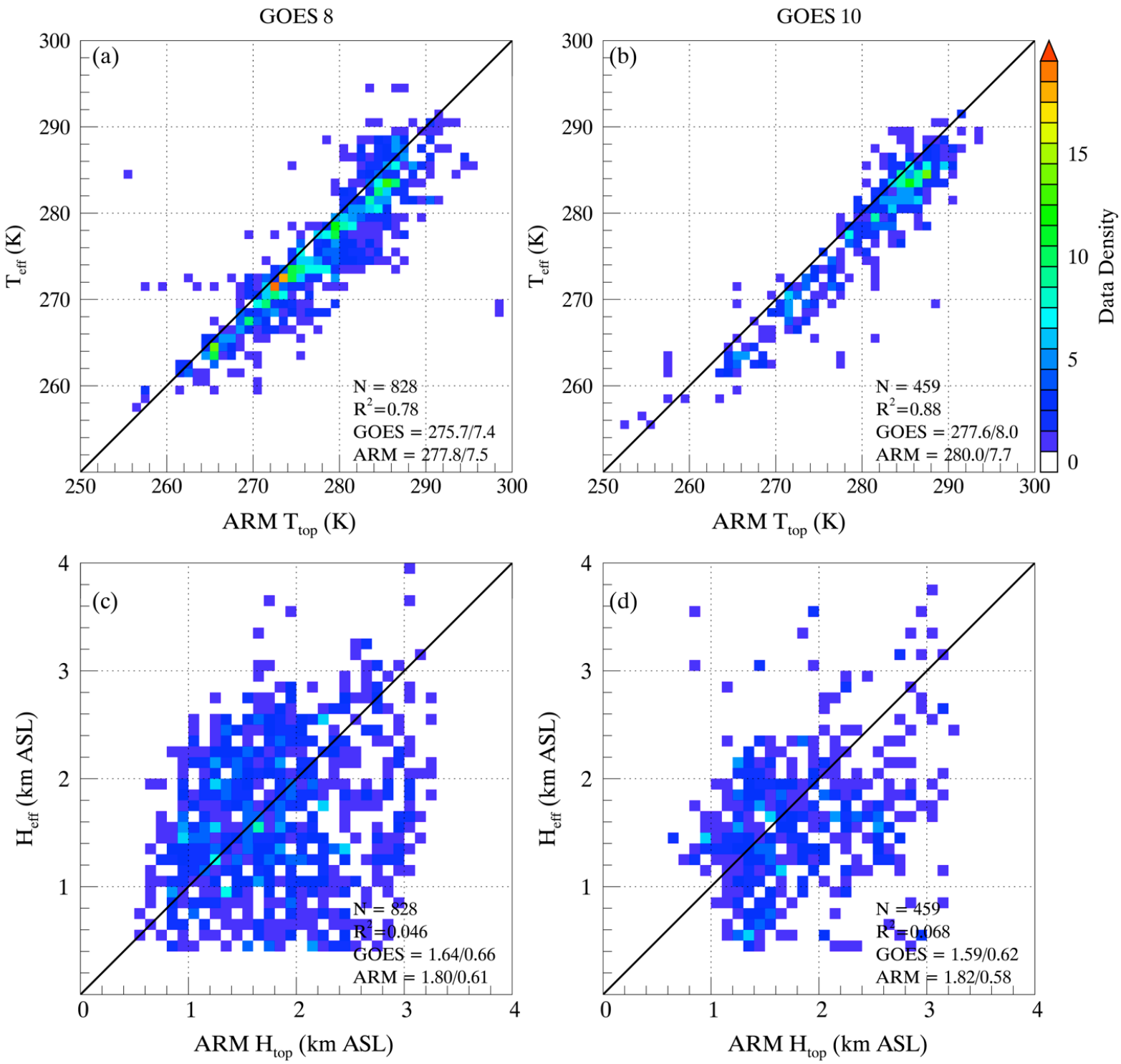
GOES 8
GOES 10
(a)
(b)
(c)
(d)
T_{eff} (K)
ARM T_{top} (K)
H_{eff} (km ASL)
ARM H_{top} (km ASL)
Data Density
N = 828
R^2=0.78
GOES = 275.7/7.4
ARM = 277.8/7.5
N = 459
R^2=0.88
GOES = 277.6/8.0
ARM = 280.0/7.7
N = 828
R^2=0.046
GOES = 1.64/0.66
ARM = 1.80/0.61
N = 459
R^2=0.068
GOES = 1.59/0.62
ARM = 1.82/0.58

		Winter		Spring		Summer		Fall		Annual	
		Mean	Std.	Mean	Std.	Mean	Std.	Mean	Std.	Mean	Std.
Cloud Base Height (km)	ARM	0.94	0.39	1.17	0.44	1.14	0.49	1.00	0.46	1.07	0.45
Cloud Top Height (km)	ARM	1.53	0.55	1.94	0.56	1.97	0.54	1.72	0.61	1.80	0.59
Cloud Eff. Height (km)	GOES	1.49	0.72	1.80	0.68	1.37	0.68	1.49	0.58	1.62	0.64
GOES H_{eff} - ARM H_{top} (km)		-0.03	0.80	-0.14	0.77	-0.62	0.58	-0.23	0.75	-0.19	0.77
Cloud Base Temp. (K)	ARM	270.8	6.5	280.4	7.0	289.3	2.7	281.4	6.2	279.5	8.1
Cloud Top Temp. (K)	ARM	271.4	6.8	279.0	6.7	286.5	2.9	280.9	6.4	278.6	7.6
Cloud Eff. Temp. (K)	GOES	268.1	5.7	277.2	6.6	284.5	4.7	278.5	6.5	276.3	7.7
ARM T_{top} - GOES T_{eff} (K)		-3.4	3.9	-1.7	3.2	-1.9	3.5	-2.3	2.9	-2.2	3.3
Effective Radius (r_e; μm)	ARM	8.1	3.0	9.1	2.9	8.9	3.6	9.1	3.9	8.9	3.3
	GOES	10.8	2.6	10.4	3.3	10.6	3.8	10.5	2.7	10.5	2.8
GOES r_e - ARM r_e (μm)		2.6	2.9	1.3	3.5	1.8	4.5	1.4	3.5	1.6	3.5
Cloud Optical Depth	ARM	25.6	16.5	28.0	19.0	29.2	20.1	29.6	18.7	28.1	18.59
	GOES	29.9	28.0	25.2	21.7	23.0	21.4	33.5	31.3	28.2	21.87
GOES τ - ARM τ		4.4	12.2	-3.2	13.1	-5.9	12.6	5.0	17.3	0.2	14.76
LWP (g m^{-2})	ARM	156.8	257.3	175.7	208.4	168.2	151.4	187.8	214.8	174.5	216.6
	GOES	213.8	226.4	164.5	156.7	154.0	162.8	231.8	235.6	191.9	167.7
GOES LWP - ARM LWP (g m^{-2})		61.6	209.9	-12.2	160.8	-11.8	112.6	51.1	186.5	19.0	178.2

		January		February		March		April		May		June	
		Mean	Std.	Mean	Std.	Mean	Std.	Mean	Std.	Mean	Std.	Mean	Std.
Cloud Base Height (km)	ARM	0.72	0.23	1.02	0.43	1.14	0.43	1.20	0.47	1.18	0.43	1.23	0.53
Cloud Top Height (km)	ARM	1.37	0.44	1.57	0.59	1.77	0.51	2.12	0.52	2.05	0.57	2.09	0.48
Cloud Eff. Height (km)	GOES	1.35	0.63	1.51	0.70	1.86	0.69	1.77	0.66	1.73	0.68	1.53	0.68
GOES H_{eff} - ARM H_{top} (km)		-0.02	0.60	-0.04	0.78	0.08	0.70	-0.33	0.76	-0.32	0.79	-0.58	0.57
Cloud Base Temp. (K)	ARM	271.5	5.4	270.4	6.3	276.2	6.3	282.0	5.9	285.4	4.7	288.6	2.7
Cloud Top Temp. (K)	ARM	272.5	5.5	270.3	7.2	275.3	6.6	280.3	5.1	283.4	4.5	285.7	2.8
Cloud Eff. Temp. (K)	GOES	269.2	4.9	267.2	5.1	273.4	5.7	278.7	5.9	281.9	4.6	283.4	5.1
GOES T_{eff} - ARM T_{top} (K)		-3.5	2.7	-3.3	5.1	-1.7	2.5	-1.7	3.2	-1.6	4.0	-2.3	3.6
Effective Radius (r_e; μm)	ARM	8.3	3.1	7.6	2.7	9.1	3.4	9.3	2.5	8.9	2.5	9.2	3.6
	GOES	11.7	2.5	10.3	2.3	10.1	2.6	10.3	3.5	11.0	4.0	10.3	3.1
GOES r_e - ARM r_e (μm)		3.4	3.0	2.8	2.9	1.1	3.4	0.9	3.2	1.9	3.8	1.2	3.1
Cloud Optical Depth	ARM	29.5	14.9	22.7	18.1	26.3	16.6	27.6	19.8	31.0	21.3	31.3	22.1
	GOES	32.9	25.8	27.6	28.3	26.4	22.4	25.3	24.0	23.0	18.1	24.2	21.6
GOES τ - ARM τ		3.1	9.5	4.9	13.4	-0.6	12.7	-3.0	13.0	-7.4	13.0	-7.3	14.1
LWP ($g\ m^{-2}$)	ARM	204.9	389.3	129.2	184.3	187.4	272.2	166.7	151.7	165.7	120.7	181.5	152.7
	GOES	258.7	231.3	190.8	220.1	171.9	161.6	159.7	161.6	156.8	143.3	161.7	172.1
GOES LWP - ARM LWP ($g\ m^{-2}$)		54.6	309.6	65.7	163.4	-14.4	215.5	-13.3	120.2	-7.7	67.3	-20.9	106.1

		July		August		September		October		November		December	
		Mean	Std.	Mean	Std.	Mean	Std.	Mean	Std.	Mean	Std.	Mean	Std.
Cloud Base Height (km)	ARM	0.86	0.28	1.33	0.43	0.96	0.30	0.93	0.43	1.12	0.57	1.04	0.38
Cloud Top Height (km)	ARM	1.65	0.58	2.14	0.42	1.93	0.56	1.47	0.51	1.90	0.64	1.64	0.58
Cloud Eff. Height (km)	GOES	0.91	0.37	1.63	0.68	1.24	0.56	1.45	0.47	1.73	0.63	1.63	0.78
ARM H_{top} - GOES H_{eff} (km)		-0.75	0.55	-0.54	0.71	-0.69	0.76	-0.03	0.68	-0.17	0.67	-0.02	0.99
Cloud Base Temp. (K)	ARM	290.8	1.7	289.2	3.1	286.3	3.5	281.2	5.4	277.9	6.5	270.7	7.9
Cloud Top Temp. (K)	ARM	288.6	2.6	285.6	1.9	286.4	3.9	280.7	5.4	276.8	5.9	271.8	7.3
Cloud Eff. Temp. (K)	GOES	287.0	2.7	285.0	4.0	283.4	4.2	278.7	5.6	274.4	6.2	268.3	6.9
GOES T_{eff} - ARM T_{top} (K)		-1.7	3.2	-0.3	3.6	-2.9	2.9	-1.8	2.8	-2.4	2.9	-3.5	3.0
Effective Radius (r_e; μm)	ARM	7.6	2.2	10.7	5.0	9.8	3.5	8.3	3.5	9.9	4.3	8.7	3.1
	GOES	11.2	5.4	10.3	2.4	10.4	2.1	10.3	2.5	10.9	3.2	10.3	2.7
GOES r_e - ARM r_e (μm)		4.1	5.7	-0.3	5.5	0.5	3.5	2.1	3.0	1.1	3.8	1.6	2.7
Cloud Optical Depth	ARM	27.9	17.9	21.0	9.7	37.2	21.9	24.1	12.1	31.9	21.4	25.6	14.7
	GOES	22.3	23.5	18.0	11.9	40.5	33.6	26.2	24.8	38.3	35.2	30.0	29.5
GOES τ - ARM τ		-3.9	10.2	-3.3	7.4	3.3	17.8	3.9	16.1	7.6	18.5	4.9	13.1
LWP (g m^{-2})	ARM	135.5	120.0	172.4	204.7	228.5	165.1	129.5	101.4	237.6	313.0	142.8	121.9
	GOES	152.6	164.3	114.1	75.4	273.4	247.0	181.6	195.7	269.8	262.9	199.8	223.5
GOES LWP - ARM LWP (g m^{-2})		30.3	69.5	-60.5	187.0	42.1	102.0	63.6	116.4	40.5	280.2	63.4	110.2

		12		13		14		15		16		17	
		Mean	Std.	Mean	Std.	Mean	Std.	Mean	Std.	Mean	Std.	Mean	Std.
Cloud Base Height (km)	ARM	0.82	0.21	1.03	0.42	1.02	0.44	0.91	0.40	0.95	0.40	1.01	0.40
Cloud Top Height (km)	ARM	1.84	0.79	1.89	0.65	1.75	0.56	1.61	0.62	1.66	0.60	1.76	0.59
Cloud Eff. Height (km)	GOES	0.66	0.31	0.93	0.46	1.09	0.58	1.22	0.61	1.58	0.65	1.80	0.61
GOES Heff - ARM H_{top} (km)		-1.18	0.97	-0.97	0.71	-0.65	0.66	-0.39	0.75	-0.08	0.74	0.03	0.76
Cloud Base Temp. (K)	ARM	288.5	5.0	284.2	6.3	280.7	8.2	278.2	8.8	279.7	8.3	279.4	8.0
Cloud Top Temp. (K)	ARM	285.2	2.7	282.1	5.9	279.7	7.9	278.6	7.6	279.0	7.5	278.8	7.5
Cloud Eff. Temp. (K)	GOES	283.7	5.4	278.6	6.7	276.7	8.0	275.2	8.0	276.4	7.9	276.5	7.7
GOES T_{eff} - ARM T_{top} (K)		-1.5	3.7	-3.2	3.2	-3.0	4.2	-3.4	4.9	-2.5	3.1	-2.1	2.9
Effective Radius (r_e; μm)	ARM	8.6	2.4	10.0	5.1	9.1	3.6	8.8	3.2	8.8	3.3	8.6	3.0
	GOES	26.0	4.4	15.1	6.1	11.7	3.9	10.5	2.2	10.6	2.2	10.1	2.2
GOES r_e - ARM r_e (μm)		18.4	4.1	5.4	7.0	2.7	3.7	1.7	3.2	1.8	3.1	1.5	2.6
Cloud Optical Depth	ARM	17.1	6.7	32.4	18.8	30.0	14.5	30.0	14.8	31.0	17.3	30.2	19.7
	GOES	3.1	2.1	25.9	31.4	28.1	28.1	30.3	27.2	28.0	23.8	27.3	23.1
GOES τ - ARM τ		-17.5	5.7	-3.7	24.8	0.3	16.8	3.2	12.1	0.7	11.4	-0.9	12.6
LWP ($g\ m^{-2}$)	ARM	84.2	77.9	201.3	203.5	168.2	118.9	160.6	126.1	161.4	140.6	181.7	275.1
	GOES	54.3	40.2	213.3	249.3	209.1	229.0	208.9	200.0	194.4	176.5	179.1	172.1
GOES LWP - ARM LWP ($g\ m^{-2}$)		-25.4	47.0	14.1	149.0	47.0	137.7	46.5	82.0	31.9	93.4	-3.1	235.7

		18		19		20		21		22		23		24	
		Mean	Std.	Mean	Std.	Mean	Std.	Mean	Std.	Mean	Std.	Mean	Std.	Mean	Std.
Cloud Base Height (km)	ARM	1.08	0.44	1.13	0.42	1.20	0.49	1.20	0.47	1.31	0.54	1.30	0.55	1.08	0.09
Cloud Top Height (km)	ARM	1.80	0.56	1.81	0.57	1.98	0.58	1.91	0.58	1.94	0.55	2.07	0.51	1.96	0.61
Cloud Eff. Height (km)	GOES	1.94	0.58	1.98	0.59	1.87	0.62	1.73	0.60	1.49	0.58	1.28	0.53	0.67	0.08
GOES Heff - ARM H_{top} (km)		0.13	0.70	0.16	0.67	-0.11	0.71	-0.19	0.66	-0.46	0.58	-0.79	0.52	-1.28	0.54
Cloud Base Temp. (K)	ARM	278.6	7.9	279.1	7.9	278.9	8.3	277.9	7.7	279.0	7.5	281.7	7.5	286.4	4.1
Cloud Top Temp. (K)	ARM	278.0	7.6	278.1	7.8	277.4	8.2	276.7	7.4	277.9	7.4	280.4	5.7	283.0	0.3
Cloud Eff. Temp. (K)	GOES	276.3	7.4	276.3	7.8	275.8	7.9	275.0	7.3	275.7	7.3	278.2	6.7	280.5	0.5
GOES T_{eff} - ARM T_{top} (K)		-1.7	3.3	-1.7	2.9	-1.6	3.0	-1.7	2.6	-2.1	2.4	-2.1	2.7	-2.6	0.5
Effective Radius (r_e; μm)	ARM	8.6	2.9	8.6	2.3	8.9	2.8	8.9	2.9	9.5	4.4	9.6	4.4	12.3	5.7
	GOES	9.5	1.9	9.5	1.9	9.9	2.4	9.5	2.2	10.6	2.2	11.7	3.4	18.6	3.0
GOES r_e - ARM r_e (μm)		0.9	2.5	0.9	2.4	0.9	2.7	0.7	2.8	1.2	4.5	2.0	3.7	6.4	6.2
Cloud Optical Depth	ARM	29.7	19.0	33.4	25.1	31.6	19.3	34.8	18.1	32.2	14.3	33.7	14.5	36.0	1.9
	GOES	24.5	20.7	24.7	22.2	29.6	26.7	31.0	26.0	36.4	36.0	34.0	35.5	48.6	37.2
GOES τ - ARM τ		-3.2	8.7	-4.2	14.8	-0.3	11.2	2.6	12.1	9.9	25.4	5.1	15.8	12.6	19.7
LWP ($g\ m^{-2}$)	ARM	167.5	241.8	150.1	131.1	210.1	347.2	173.4	148.8	180.3	177.4	229.7	379.7	283.5	144.6
	GOES	152.5	145.9	152.5	152.5	196.3	203.9	201.1	196.3	254.8	273.8	254.5	280.5	562.5	409.3
GOES LWP - ARM LWP ($g\ m^{-2}$)		-13.6	189.7	3.2	83.9	-7.7	264.8	30.8	113.7	79.1	205.0	20.3	325.0	279.0	72.1